H2020 Grant Agreement N° 690835

Deliverable D1.2 – WP1 – Due date: 31 December 2017

Title: Report on g-2 trackers

Type: Report

Dissemination level: Public

WP number: WP1

Lead Beneficiary: LIVERPOOL

Report on the Installation and Initial Commissioning of the g-2 Tracker Detector.

1. Introduction.

The new muon g-2 experiment at Fermilab, E989 is designed to measure the anomalous magnetic moment of the muon to unprecedented precision. It is an improved version of the E821 experiment at Brookhaven, which measured the anomalous magnetic moment to be greater than 3 standard deviations away from the theoretically predicted value. This intriguing discrepancy could hint at new physics phenomena and made the case for the current experiment compelling. With the expected increase of a factor ~20 in statistics and the improvements in the detector design, E989 will have the precision to definitively search for new physics processes contributing to the anomalous magnetic moment. The experiment is now entering the data taking phase, with first results anticipated in 2018. The track detectors, which form the subject of this report have been successfully built, tested, installed and commissioned in time for this exciting phase.

2. General overview on the contributions of the trackers to the experiment.

The muon ring from E821 was transported from Brookhaven to Fermilab. 24 Calorimeters are spaced evenly around to ring to measure the energies of positrons arising from the positive muon decays.

As part of the improvements in the detector, new tracking detectors were designed and built at the University of Liverpool. Two trackers are currently installed in the experiment in front of calorimeter 15 (~ 7 o'clock position) and calorimeter 21 (~10 o'clock position), as shown in Figure 1. Each of the trackers consists of eight tracker modules, positioned so as to provide optimum coverage for muon decay positrons approaching the calorimeter.

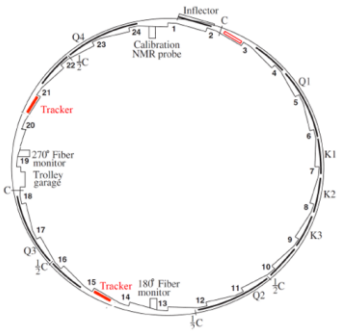

Figure 1: Outline of tracker positions.

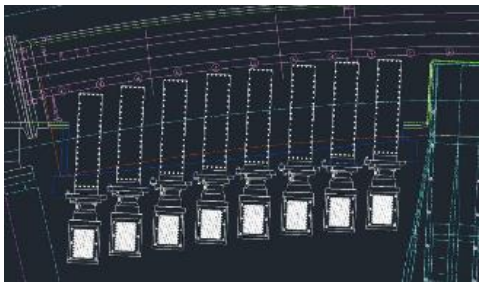

Figure 2: Positions of the 8 tracker modules.

Each tracker module contains 128 aluminized mylar straws arranged in 4 layers, each of 32 individual straws. As summarised in Figure 3, the length of each straw is 10 cm, with 2 layers tilted at +7.5 degrees and 2 at – 7.5 degrees to the vertical, to provide track reconstruction in the vertical direction. Each straw contains a 25 micron diameter, centrally located, gold-plated tungsten wire at ~1700 Volts to detect signals from drifting electrons in the 50:50 Argon/Ethane gas in the straws.

Straw material	Aluminized Mylar
Straw wall thickness	15 μm
Wire	25 μm gold-plated tungsten
Straw length	10 cm
Stereo angle	$\pm$ 7.5° from vertical
Gas	50:50 Argon:Ethane
Pressure	1 Atm
Operating voltage	1800 V

Figure 3: Summary of tracker straw design.

The trackers are designed to make three substantial contributions to the experiment:

1. By reconstructing the trajectories of the decay positrons we can extrapolate back to ascertain the muon decay positions and thus, build up an accurate picture of the muon beam profile as a function of time. Not only will this allow the optimisation of the incoming muon beam, but will also allow us to measure beam oscillation parameters.

2. One of the potential problems occurs if two positrons enter a calorimeter within a short time period and are badly reconstructed. The pileup correction applied to the calorimeter energies to adjust for this can be verified by studying cases in which the trackers confirm the presence of two positrons. In addition the comparison of reconstructed positron momenta with their reconstructed calorimeter energies allows confirmation that the calorimeters are well calibrated.

3. The third major contribution of the trackers involves identifying any tilt in the muon precession plane away from vertical. Such a tilt would be indicative of a muon electric dipole moment. A tracker based search for a muon electric dipole moment is expected to lower the upper limit on the electric dipole moment by several orders of magnitude and will test the predictions of Beyond Standard Model physics predictions.

The role of the trackers is summarised in Figure 4, where the expected improvement over E821 is outlined.

Uncertainty	E821 value	E989 goal	Role of tracking
Magnetic field seen by muons	0.03 ppm	0.01 ppm	Measure beam profile on a fill by fill basis ensuring proper muon beam alignment
Beam dynamics corrections	0.05 ppm	0.03 ppm	Measure beam oscillation parameters as a function of time in the fill
Pileup correction	0.08 ppm	0.04 ppm	Isolate time windows with more than one positron hitting the calorimeter to verify calorimeter based pileup correction
Calorimeter gain stability	0.12 ppm	0.02 ppm	Measure positron momentum with better resolution than the calorimeter to verify calorimeter based gain measurement
Precession plane tilt	4.4 μRad	0.4 μRad	Measure up-down asymmetry in positron decay angle

Figure 4: The contribution of the trackers to the experimental goals of E989.

3. Construction of tracker modules.

The tracker modules themselves have been constructed in Liverpool, where the necessary workshop and cleanroom facilities exist. The readout electronics for the detectors was developed in Boston and the associated DAQ software at UCL. The components needed for each module are shown in Figure 5.

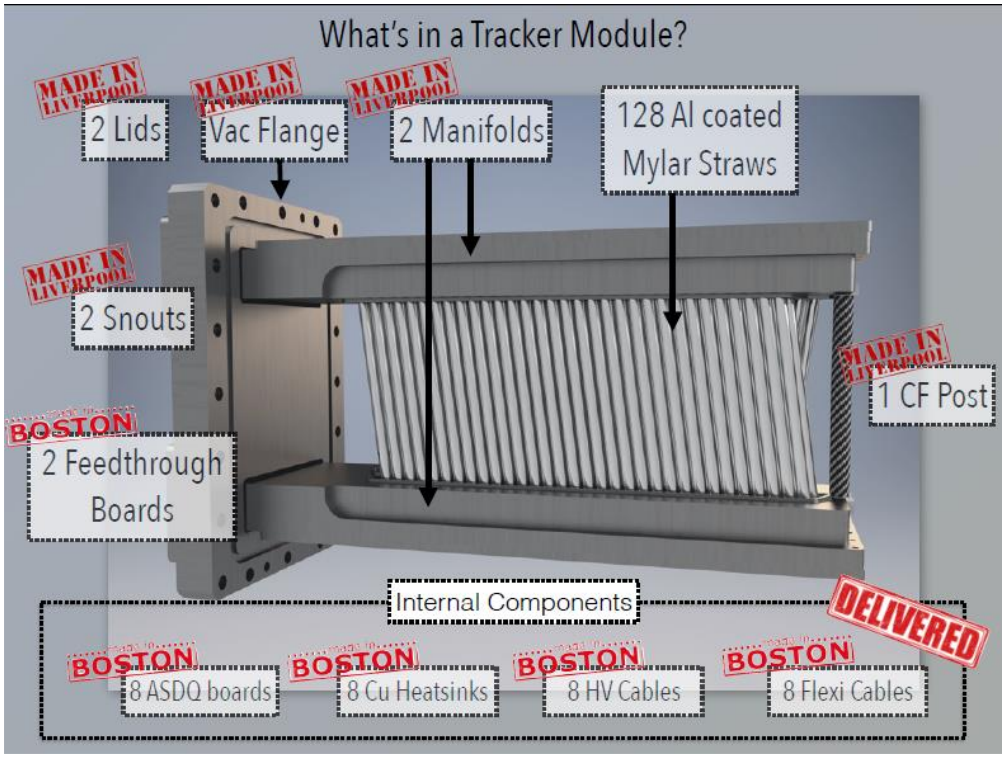

Figure 5: An illustration of the components of a tracker module.

Mechanical Workshop.

The modules begin their long journey in the mechanical workshop at Liverpool, where the top and bottom manifolds, vacuum flange, module lids and end snouts are fabricated. The Liverpool workshop hosts two computer operated milling machines which were programmed to rough out the initial manifold blocks and straw holes. Additional features, such as the various screw holes were then added and the straw holes de-burred. The total of 52 manifolds (enough for 3 trackers plus 2 spare modules) were produced at the rate of 2 per week.

Some pictures of the various stages of the mechanical production are included in Figure 6.

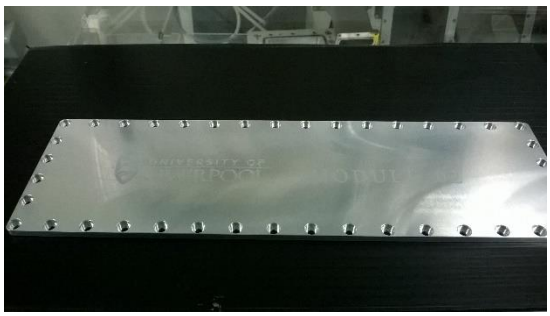

Figure 6: Production of tracker module manifolds, lids and snouts in the Liverpool workshop.

Metrology.

Upon completion in the workshop, the mechanical components of a module enter the cleanroom area and undergo complete metrology measurements using a state of the art Coordinate Measuring Machine (CMM). This device is fully programmable and takes about 45 minutes to complete all measurements on a single manifold. All features of each manifold are measured to an accuracy of approximately 10 microns at 22C, thus ensuring all used manifolds adhere to specification tolerances. Some examples of manifolds undergoing metrology are shown in Figure 7. Figure 8 shows an illustration of measurements of straw hole diameters with the allowed tolerances highlighted.

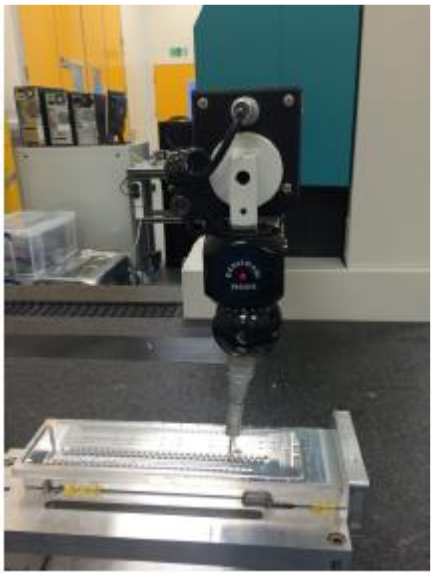

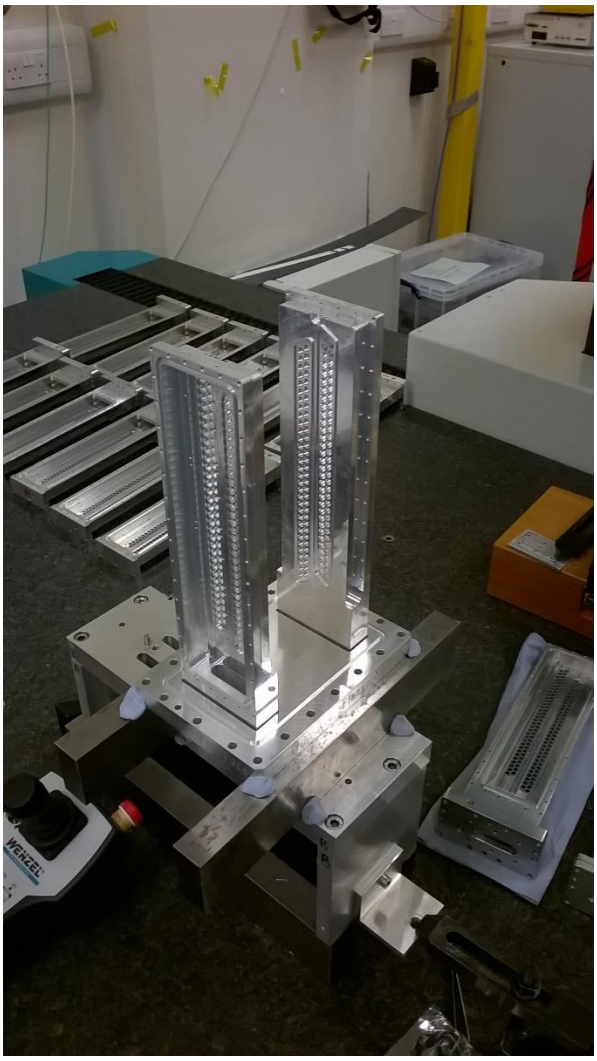

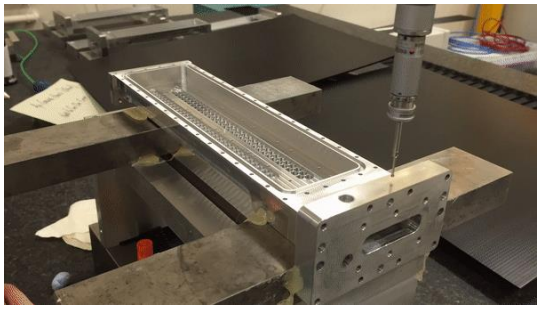

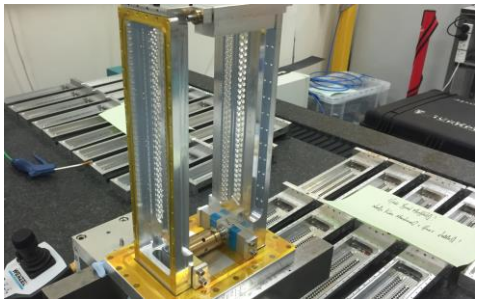

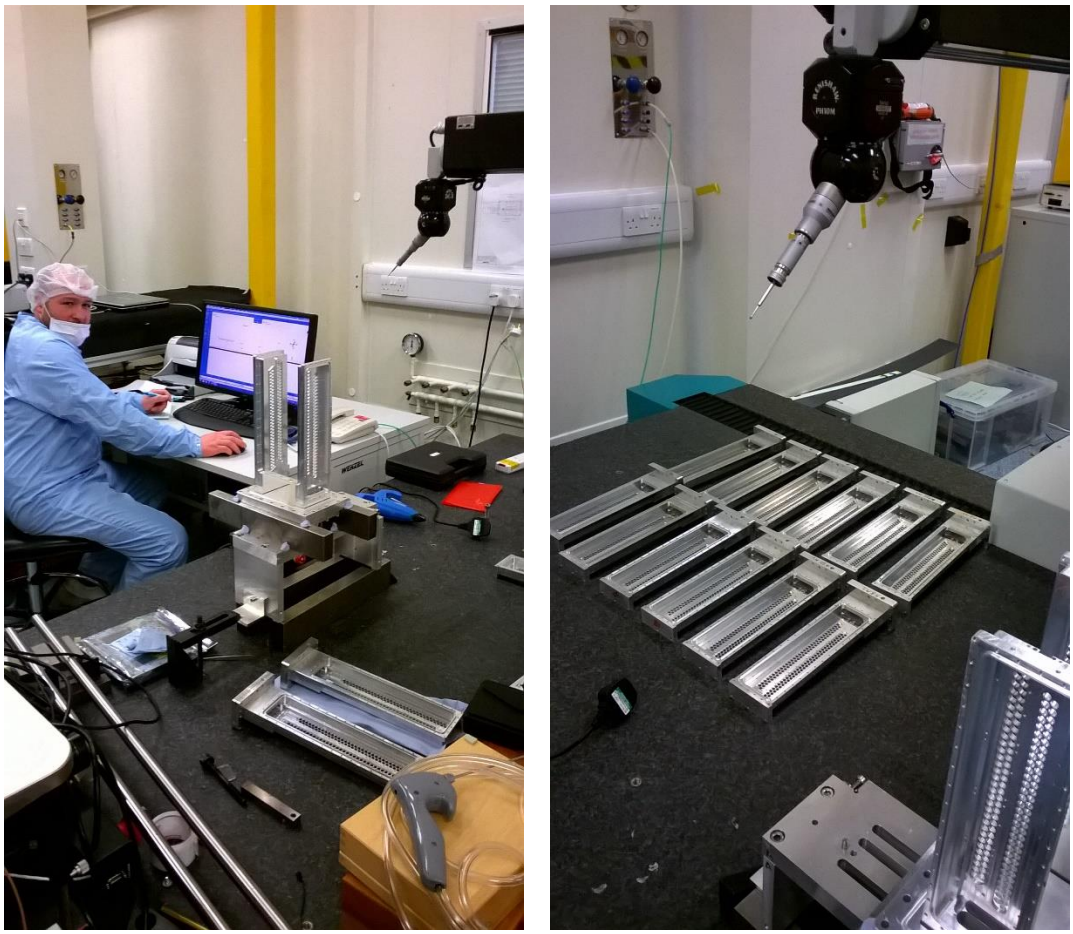

Figure 7: Module manifolds on the Coordinate Measuring Machine at Liverpool.

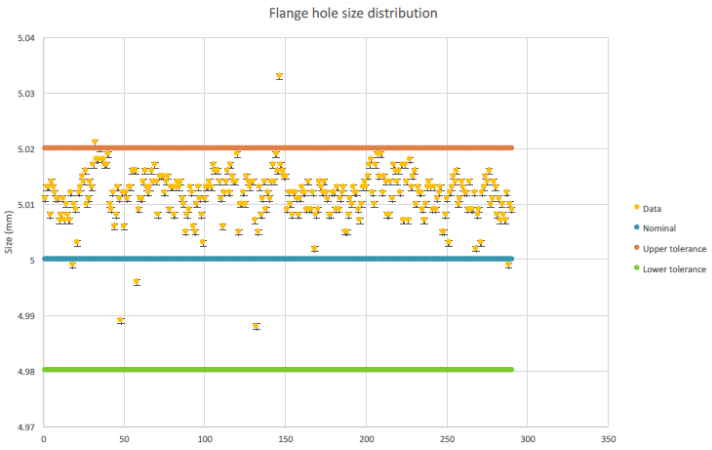

Figure 8: Measured flange hole diameters with allowed tolerances.

The metrology process yielded a pass rate of 95% for straw hole diameters, 99% for flange holes and 81% for dowel holes. After metrology, manifold and lid pairs were selected for each of the modules and initial assembly performed. The appearance of the module at this stage is shown in Figure 9.

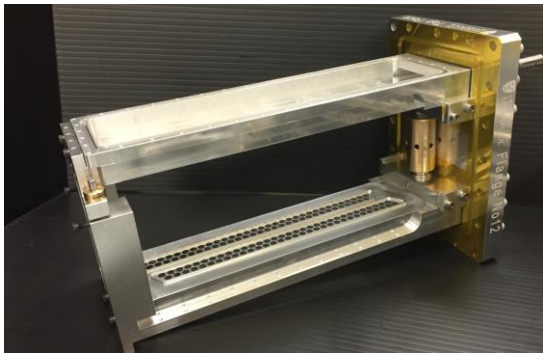

Figure 9: Initial module assembly.

Straws Leak Testing.

Before the module can be populated with straws it was necessary to select straws with an acceptable gas leak rate. This was particularly important since the straws are positioned in the beampipe and must not degrade the vacuum.

Two leak testing chambers (see Figure 10) were assembled in Liverpool and the leak rate of long straws (as they arrive in Liverpool before cutting) was measured using a 50:50 Ar/CO_2 gas mixture.

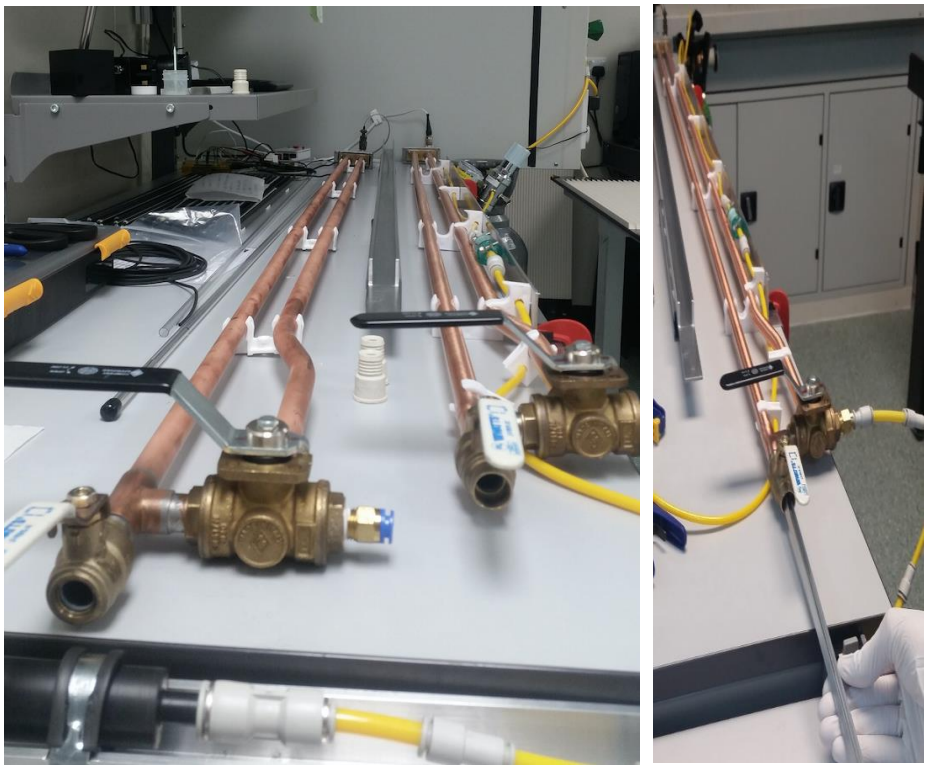

Figure 10: The 2 leak testing stations with (right) a long straw being inserted.

To be accepted the straw leak rate had to be less than 4×10^{-4} cc/min which is equivalent to 5×10^{-6} torr litres/second. The pass rate for the straws was 80%.

Module Assembly.

Long straws that passed the leak rate acceptability test were then guillotined to an exact length of 90.6 mm, aluminium endpieces glued to the straws with silver epoxy (Figure 13) and stored (see Figure 11) ready for populating the module. Every straw was also tested to check that its resistance was less than 30 Ohms, in order to avoid noisy channels.

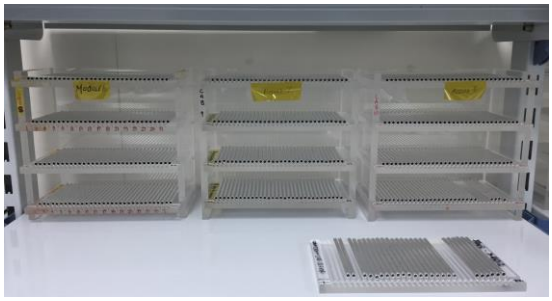

Figure 11: Cut Straws awaiting a module.

Figure 12: Straw ends glued into manifolds.

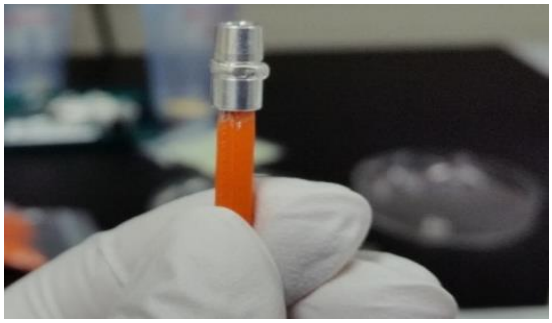

Figure 13: Gluing of aluminium endpiece.

The straws were glued into the manifolds using Araldite 20:20 glue to provide a gas seal. This was applied by hand by syringe. This process takes about one week, since the glue applied to one manifold has to cure before rotating the module to apply glue to the other manifold. The process was parallelised so that two modules could be assembled simultaneously.

Once a module had been populated with straws it was ready for wire stringing. The stringing procedure started with the threading of the 25 micron tungsten wire through the long pins and crimping. A tray of crimped wires is shown in Figure 14.

Figure 14: Crimped wires ready for insertion.

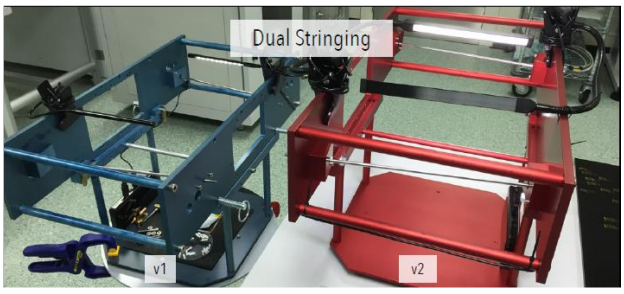

Figure 15: Module stringing jigs.

With the module held in the stringing jig, the wire is threaded through the straw and pre-tensioned to 30 grams. The short pin is then threaded on to the wire and crimped into position. Once the wires have all been crimped into position, the module is jacked apart by 70 microns to create 50 grams of

tension in the wires. Pictures illustrating the procedure are shown in Figure 16. To ascertain that the wires were correctly inserted each wire was tension tested and those failing the test were replaced.

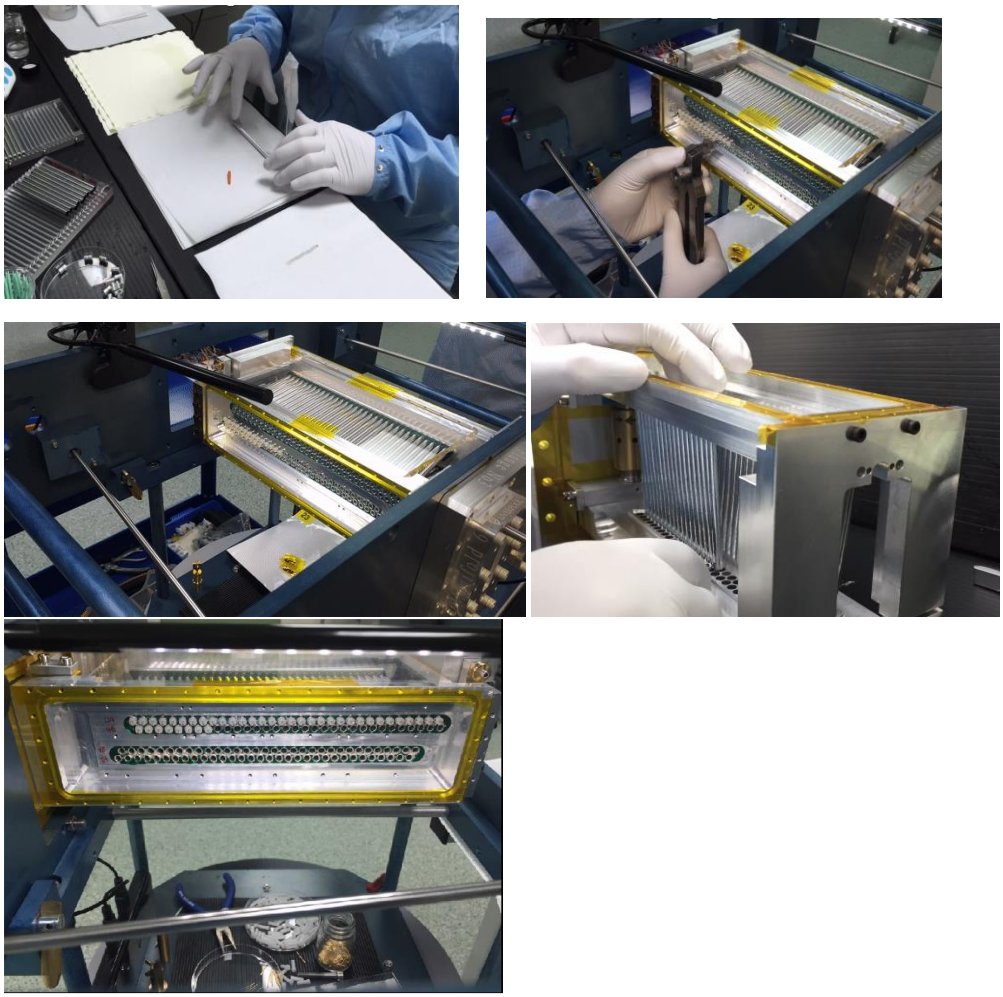

Figure 16: Stringing wires into a module.

Finally a carbon fibre post (Figure 17) was added to each module for stability.

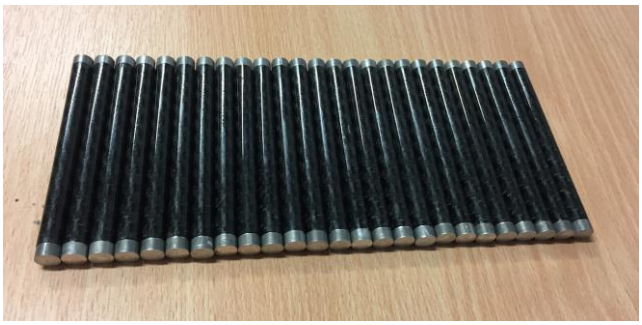

Figure 17: Carbon fibre posts, one of which was added to each module.

Addition of readout electronics.

The module manifolds contain readout electronics, designed by the Boston group to receive the raw signals from the straws. 8 ASDQs (on 4 boards) provide pulse shaping and signal discrimination, giving digital output signals. Power to and signals from the ASDQs are routed via flexicables to a feedthrough board which also acts as a gas seal. The implementation of the onboard electronics is

summarised in Figure 18. The feedthrough board acts as the backplane to the various boards outside of the vacuum, housed in the “flobber”. There is 1 HV board, 2 TDC boards and various logic boards to buffer and send the data from the TDCs.

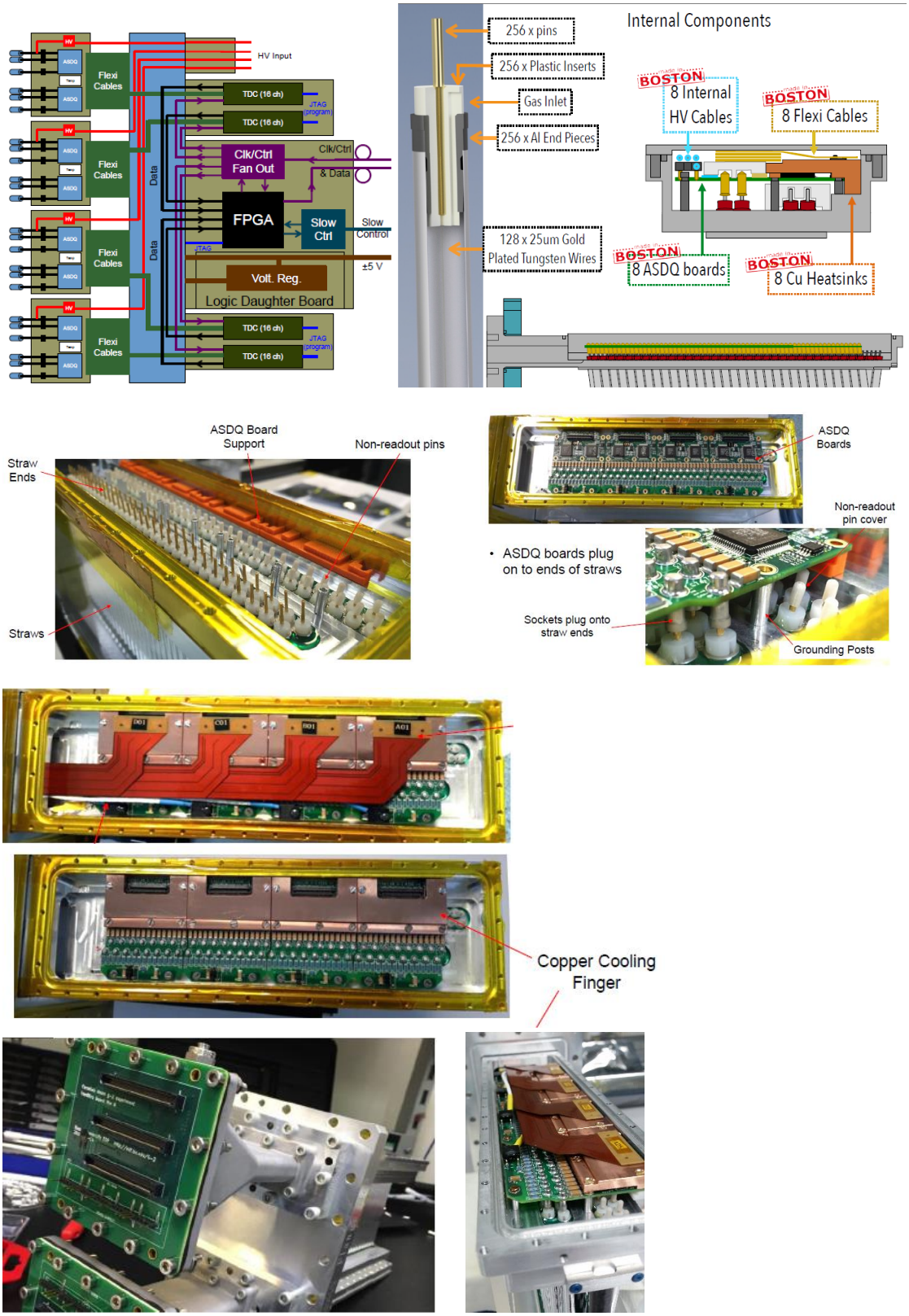

Figure 18: Various components of the tracker readout electronics. ASDQs plug onto the straw pins. Flexicables take the signals to the feedthrough board and then on to the TDCs and readout logic.

Since the tracker modules are located in vacuum inside the beampipe, a method is needed to transport away the heat produced by the onboard readout electronics. This is achieved by a copper cooling bar attached to the water based manifold cooling. A completed module and two module construction gurus are shown in Figure 19.

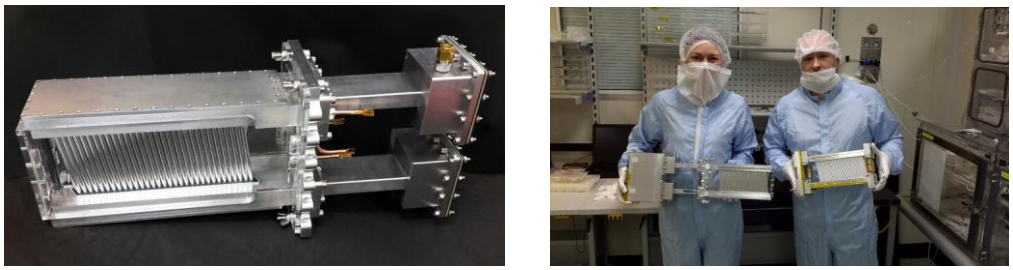

Figure 19: A completed module and two of the principal module construction experts.

Quality Assurance tests in Liverpool.

The modules are fully assembled in Liverpool and then undergo Quality Assurance tests prior to shipment to Fermilab. Initially these involve a search for gas leaks that would compromise the beampipe vacuum. Each module is inserted into the vacuum tank in Liverpool and pumped down over a period of several days. It is considered acceptable if the vacuum reaches a level of ~1 x 10^{-6} Torr. An example of a leak test is shown in Figure 20. The achieved vacuum is well below 10^{-6} Torr.

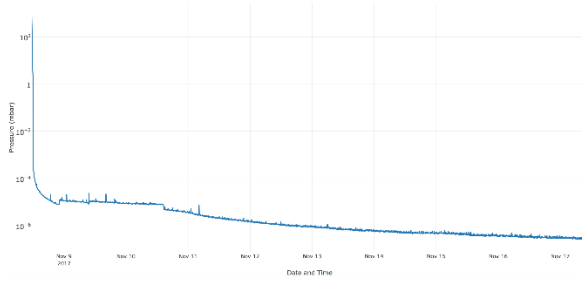

Figure 20: Example of a vacuum leak test.

Noise scans are then made to confirm that internal electronic connections are correct. HV is provided by exactly the same HV unit (Caen SY127) that will be used in the experiment. The HV is ramped up to 1500V for 24 hours with a trip current of 1 microamp. All channels ramped up successfully without the need for "training".

Finally long cosmic ray runs and source data are taken, using precisely the same DAQ setup as for the real experiment. The experimental setup in Liverpool is shown in Figure 21. The vacuum tank containing a module is on the left and the readout is on the right. The bottom right plot shows a hit map indicating that all 32 straws in all 4 layers of the module are active.

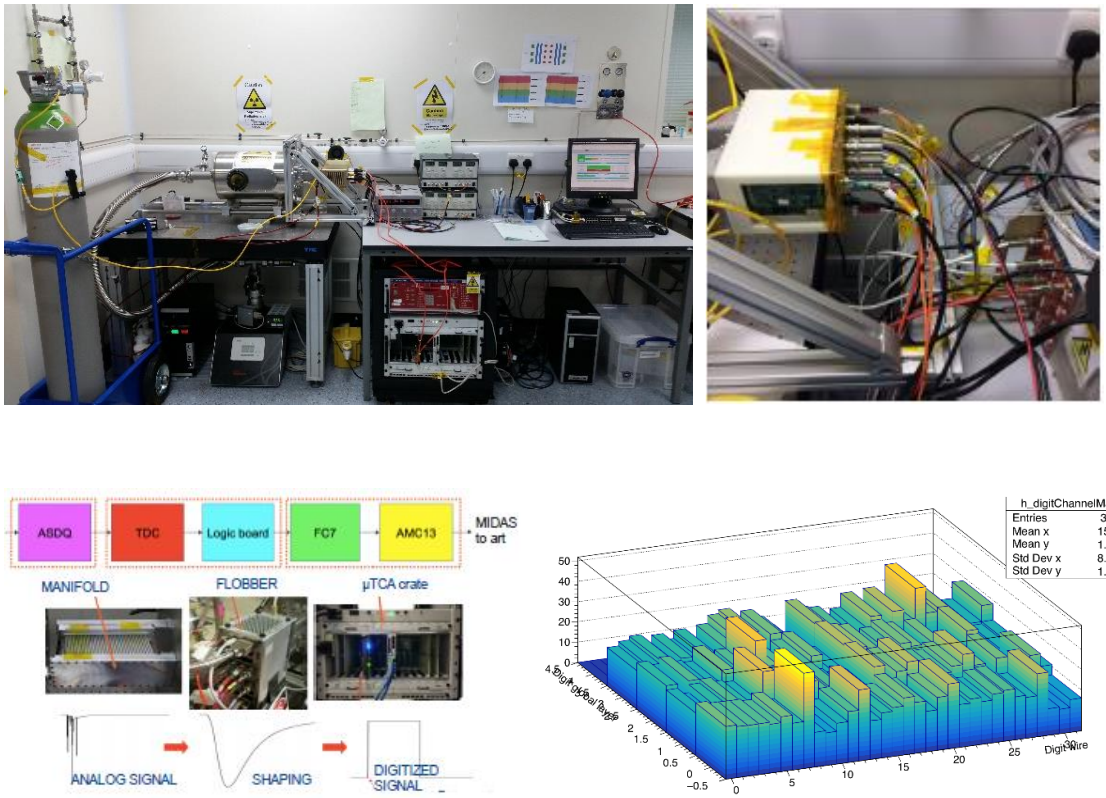

Figure 21: The Liverpool experimental setup for cosmic and source data taking.

In summary, out of the 2048 straws comprising the 16 tracker modules of the two trackers currently installed in the experiment, just 7 straws are non-functional. In addition, two spare tracker modules have been completed and are ready for use should it be necessary.

The tracker modules are quite delicate and have been transported individually to Fermilab by plane as hand luggage in specially constructed pelicases.

4. Reception tests on arrival on Fermilab.

Upon arrival at Fermilab the module undergoes an exact copy of the QA tests performed at Liverpool, in order to ascertain that no damage has been incurred during the transport. These tests are carried out under clean conditions in Lab 3, a picture of which is shown in Figure 22.

Figure 22: Lab 3 at Fermilab, where module QA tests are repeated upon arrival.

Vacuum tests.

In order to check the module has survived the flight, vacuum "rate of rise" tests are performed for various gases – Ar/C_2H_6 , CO_2 , N_2. This also provides confirmation that the module meets the requirements for vacuum integrity. A great deal of work went into understanding the leak rates for various gases, which are not the same due to their different molecular compositions. In practice the leak rate for Argon/Ethane, which is used in the experiment, is a factor of ~20 lower than that for CO_2.

Having passed the vacuum tests, module data is taken in a cosmic test stand with the module placed for optimal cosmic acceptance. This cosmic test stand is shown in Figure 23.

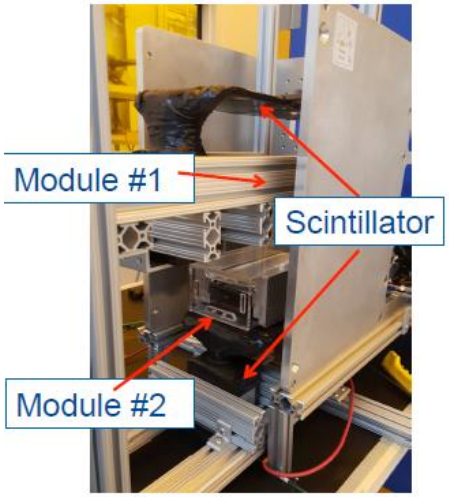

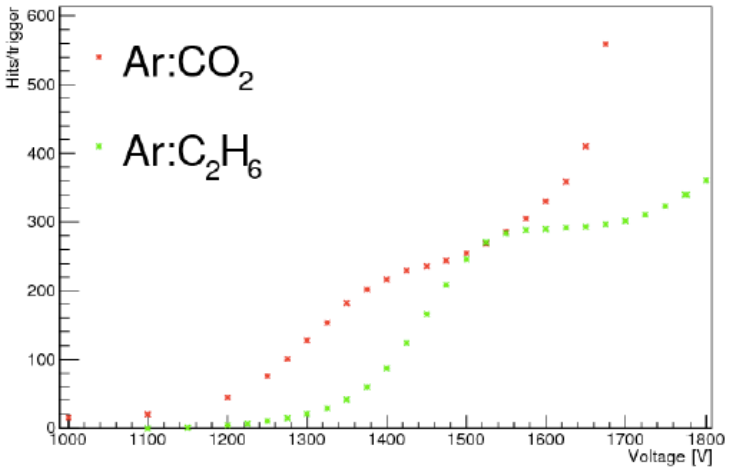

Figure 23: The cosmic test stand in Lab 3. **Figure 24: Determination of plateau regions.**

In the cosmic test stand there is sufficient space for 3 modules, with triggering and t0 provided by scintillators. As well as providing data for understanding module performance, the Lab 3 tests provided a full test of the DAQ system and track reconstruction software in the full offline software chain. As well as cosmic data, Sr_{90} source data was also recorded and used to identify the voltage plateau regions for several gases (Figure 24). On this basis it was decided to run the modules in the experiment at 1650 Volts.

In addition to the cosmic test stand, a dedicated source test stand was also available for more precise position/time measurements (Figure 25).

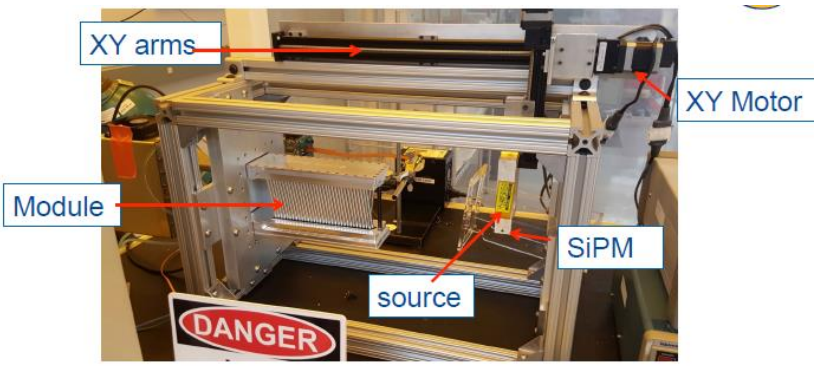

Figure 25: The source test stand in Lab 3.

Using the source stand, precise scans across the module in 6 micron steps can be performed. As an example of the source stand data, Figure 26 shows data from a single straw, in which the 7.5 degree tilt as a function of height is clearly visible.

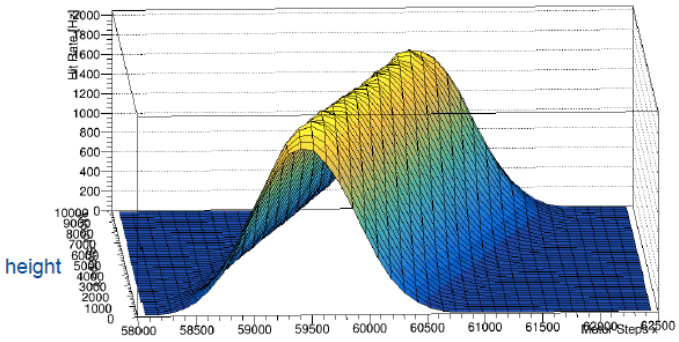

Figure 26: Source data from a single straw versus height.

5. Installation in the Ring.

The first stage of module installation in the experiment is transport across Fermilab from Lab 3 to MC1, the experimental building. This is carried out using specially adapted pelicases, through which nitrogen is flushed for several hours, to prevent a buildup of humidity on the modules themselves. The modules are then transported in the nitrogen sealed pelicases across campus. This ensures that the modules have minimal exposure to the atmosphere and are perfectly dry on insertion into the ring vacuum. The Commissioning Run for g-2 began in June 2017, by which time one full tracker (8 modules) had been installed. Some pictures from the installation are shown in Figure 27.

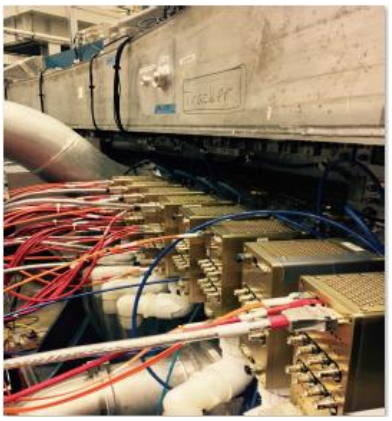

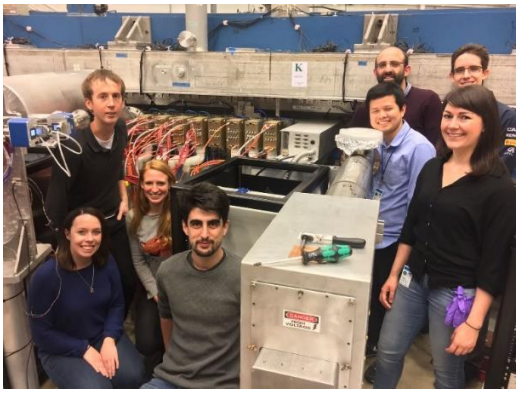

Figure 27: Installation of the first complete tracker prior to the 2017 Commissioning Run.

Since the Commissioning Run, a second full tracker has been installed in the experiment, both trackers being shown in Figure 28. Also shown is a picture from inside the beampipe of tracker modules in situ ready for beam. The stabilising carbon fibre post is clearly visible. Both trackers are now fully operational in the first g-2 Physics Runs. Both trackers are fully cabled, fully supplied with 50:50 Argon/Ethane gas and fully supplied with water coolant.

Figure 28: Pictures of the two fully installed trackers.

6. Commissioning.

One of the first things to ensure once the trackers were installed was that the vacuum in the beampipe was not compromisedby their presence. Figure 29 shows the vacuum at 3 locations in the ring over a one week period in November 2017. The blue and green curves correspond to the two tracker locations and indicate that the vacuum is acceptable in the presence of the trackers.

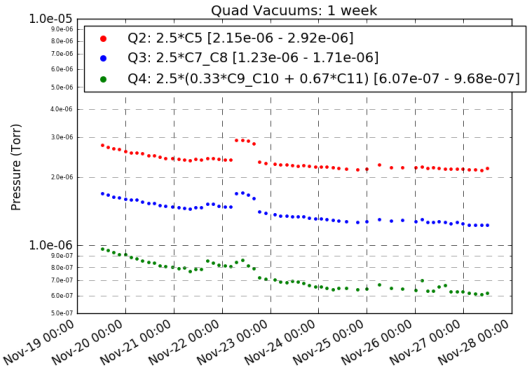

Figure 29: Beampipe vacuum, Nov 2017.

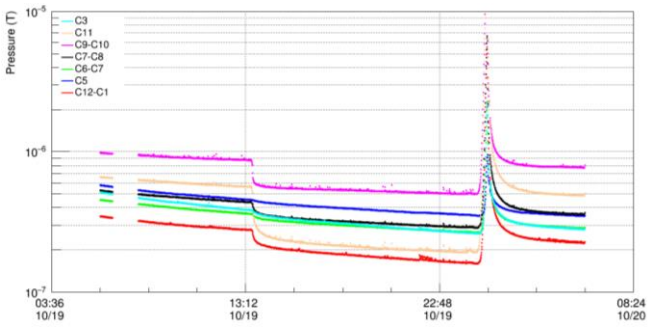

Figure 30: Vacuum improvement from cryopumps.

However, the vacuum can be further improved by the installation of cryopumps at critical locations around the ring (Figure 30). Tests indicate that a 40% improvement can be achieved. Cryopumps are currently being commissioned and will shortly be installed in the ring.

The tracker DAQ system is fully operational (Figure 31) and all modules are successfully taking data. Figure 31 also shows a tracker hit map obtained during the Commissioning Run. All straws are registering hits and as expected, those closest to the beam see the highest number of hits.

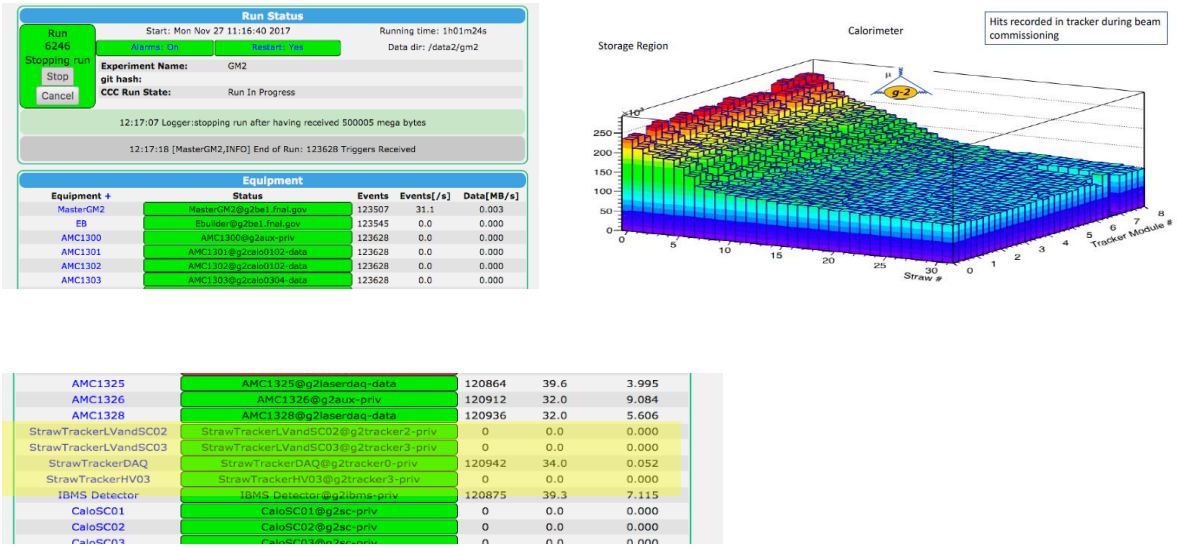

Figure 31: Illustration of the Tracker DAQ system and tracker hit map from Commissioning Run.

Displays are also being developed for the use of shift personel for tracker performance monitoring. These displays will range from simple channel on/off indicators as well as more sophisticated plots obtained by running the full reconstruction chain on a subsample of events during data taking. An example display of the water cooling and vacuum status is shown in Figure 32.

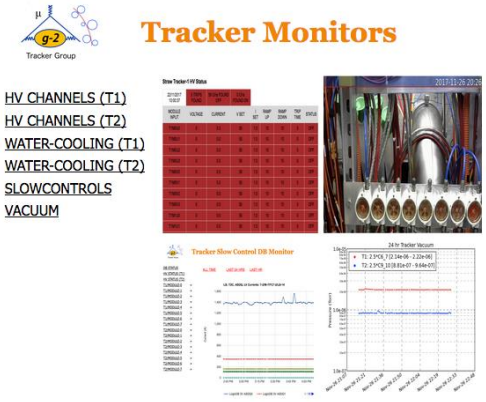

Figure 32: Example online tracker display.

Track reconstruction.

The reconstruction of tracks in the experiment is complicated by the fact that there is a large variation of the magnetic field in the region of the trackers. As a result of this, a simple helix fit to the

track is insufficient. A further complication arises from the fact that there is no defined interaction point and the T0 offset has to be determined on a track by track basis. The first stage of track finding consists of forming “time islands” of ~60 nanoseconds in length. Hits occurring within a time island could physically have arisen from the same track since the maximum drift time of electrons in the straws is ~ 60 nanoseconds. The next stage of track finding clusters together hits which could reasonably go together as one track candidate. Typically there is just one track candidate per time island, but this is not always the case and care has been taken to deal correctly with cases of more than one candidate per time island.

Hits that have been identified as forming a track candidate are passed to the track fitting stage. This uses the Geane package from CERN for accurate error propagation. Track fitting starts by making a reasonable guess at the 5 track parameters. The extrapolated track is propagated through the detector and compared to the measurements in each layer, taking into account correct error propagation from the known material map of the detector. A χ^2 minimisation is performed to ascertain the track parameters that give best agreement between measurements and predictions in each layer. An example of a fitted track is shown in Figure 33.

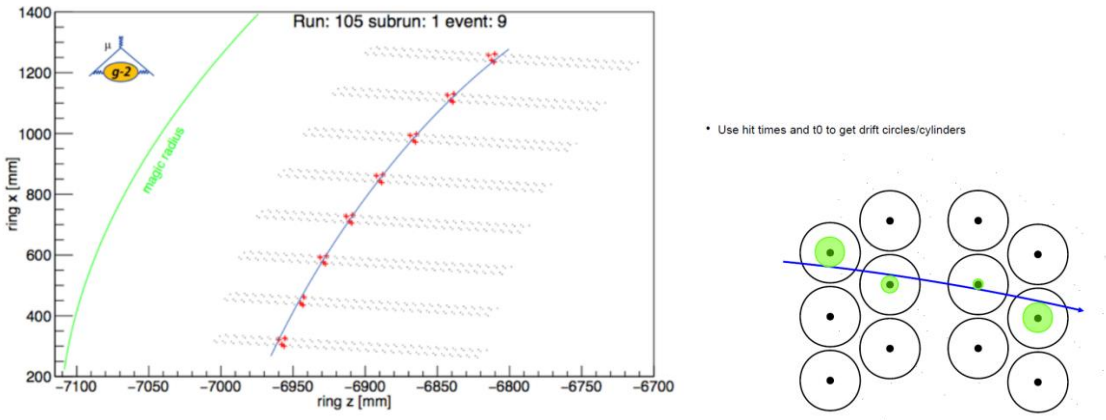

Figure 33: Example of a fitted track.

By comparing the fitted track to detector measurements the efficiency of the straws is found to be close to 100% across the full width of the straw (see Figure 34). In addition by comparing the fitted track trajectory with the drift time in a straw, the time-distance curve for electron drift in the straws can be determined. This is found to be in close agreement with Garfield based simulations of the straws (Figure 35).

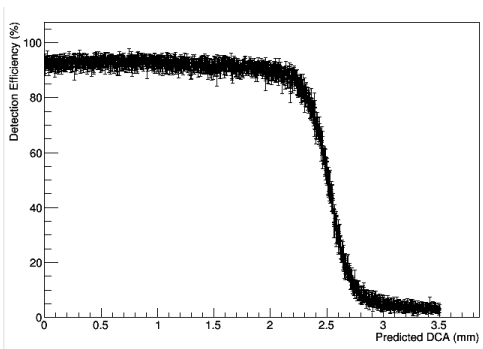

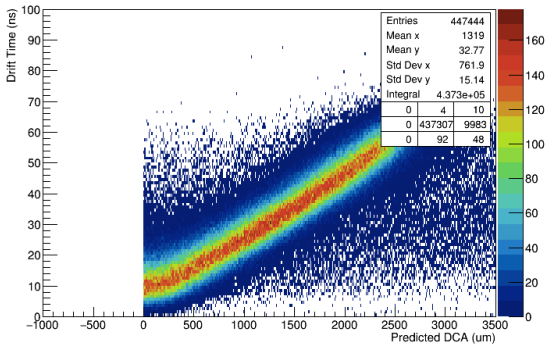

Figure 34: Straw efficiency versus drift distance. **Fig 35: Distance to straw wire versus drift time.**

Track extrapolation to determine the beam profile.

Having determined the fitted parameters for a track we are in a position to extrapolate the track backwards to estimate the muon decay point that gave rise to the observed positron, as illustrated in Figure 36.

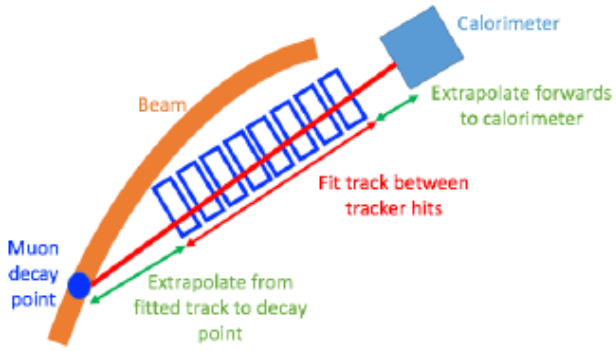

Figure 36: Schematic of muon decay point determination.

The track parameters are defined at the first layer of the tracker. From there a fourth order Runge-Kutta algorithm is used to swim the track backwards through the varying magnetic field. The step length is optimised at each stage of the extrapolation procedure depending on the field gradient at that location and is halted once the point of radial tangency (when the radial momentum component is zero) is reached, as shown in Figure 37.

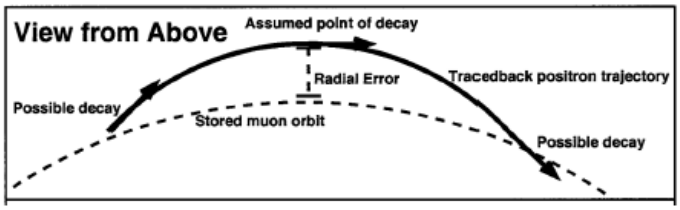

Figure 37: Schematic of point of radial tangency.

This procedure yields a consistent over estimate of the decay point radius, together with two actual possible decay positions. Simulations were used to study the corrections that had to be applied to the radial decay point estimate. It was determined that a momentum independent correction of 1.1 mm was needed to give the correct radius estimate (Figures 38 and 39).

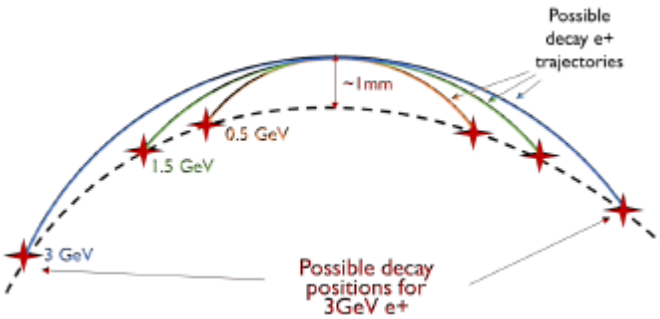

Figure 38: Illustration of possible decay points for positrons of different momenta.

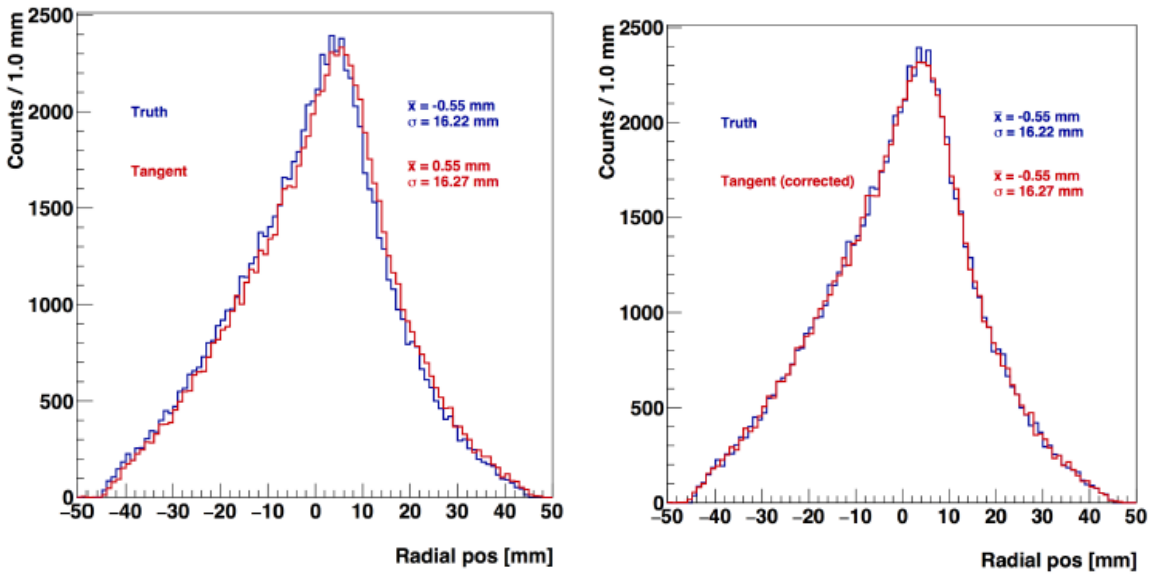

Figure 39: Comparison of radius estimate and truth before and after correction by ~1.1 mm

A full unfolding procedure for the radial estimate was also investigated but found to be unnecessary. Figure 40 shows the beamspot determination as applied to simulated muon decays (left) and for Commissioning Run data (right).

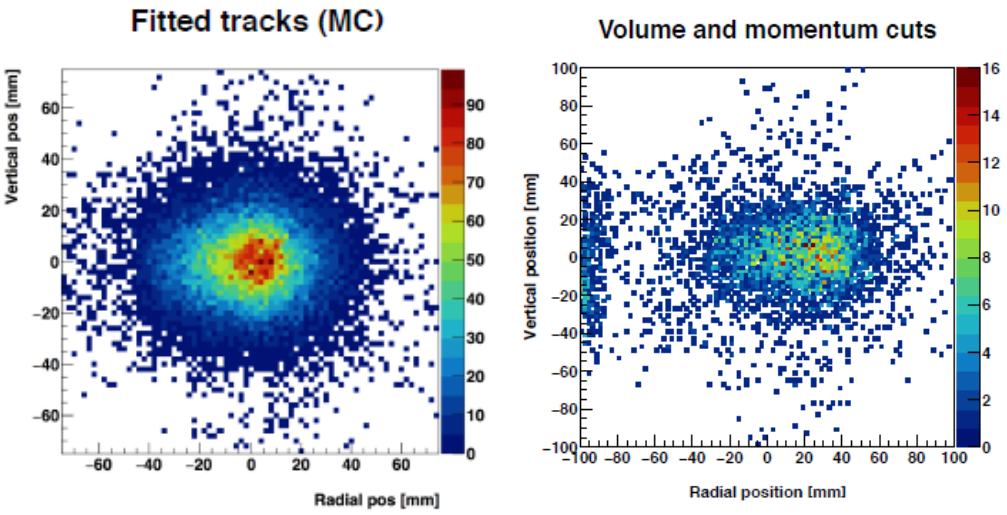

Figure 40: Beamspot determination from simulation (left) and Commissioning Run (right).

In Figure 41 a preliminary estimate for the beamspot in the most recent (Dec 17) data is shown. Fig 41a shows the radial versus vertical position for each estimated decay, Fig 41b shows the actual estimated decay position around the ring, clearly showing the acceptance region for each tracker. Figure 41c indicates the arc length from tracker to decay point as a function of positron momentum.

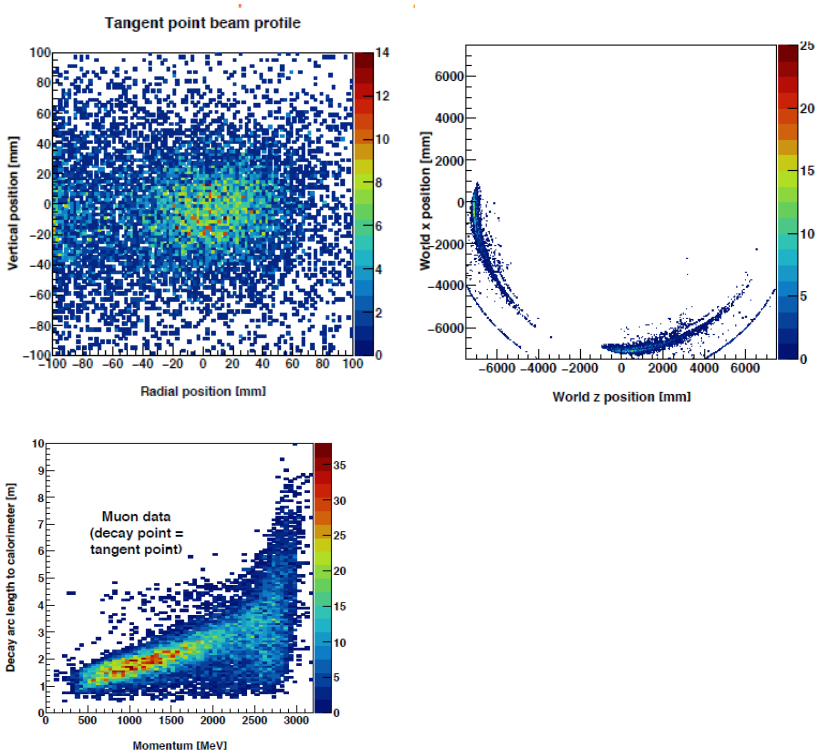

Figure 41: (a) Radial v Vertical decay point estimate. (b) Estimated decay position around the ring. (c) Arc length to the decay point v track momentum.

We are now in a position to provide valuable beam profile information, which can be used as a real time beam diagnostic tool. We can now start to make beam dynamics related studies that will help to reduce significantly the systematic errors on the measurement of g-2. To illustrate this Figure 42 shows the distribution of y (vertical position at point of radial tangency) versus y' (vertical momentum at the same point), for simulated positrons (left) and recent data (right).

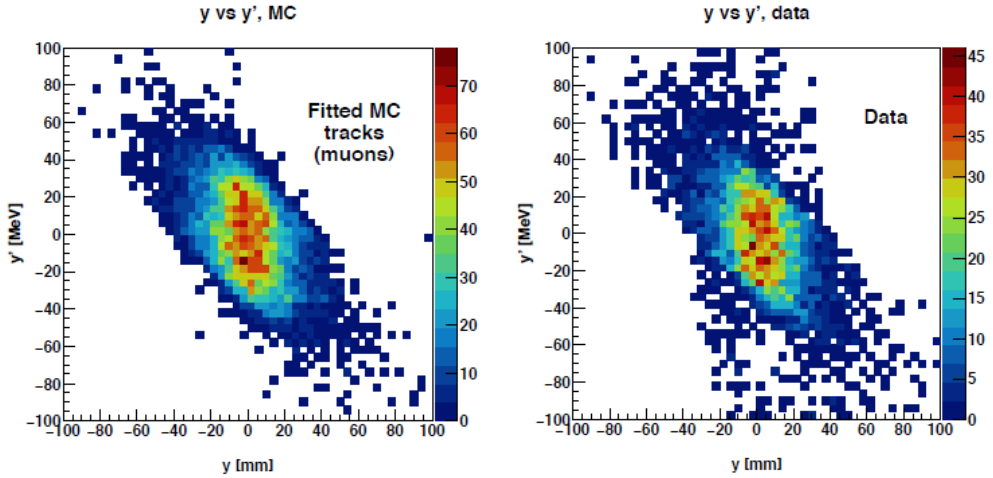

Figure 42: Distribution of vertical position versus vertical momentum at point of radial tangency. The left plot is for simulated muon decays, whilst that on the right is for recent data.

Track matching with calorimeter clusters.

As well as extrapolating back to the muon decay point, the fitted tracks can be extrapolated forwards to determine their point of entry into the calorimeter, as depicted in Figure 43.

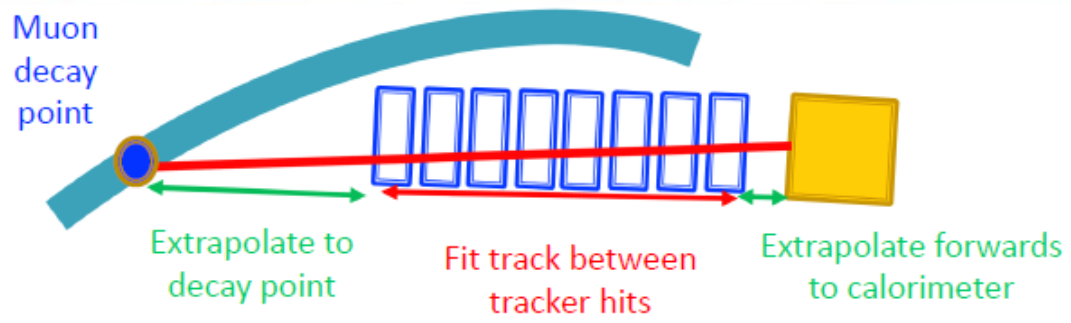

Figure 43: Schematic of track extrapolation forward to the calorimeter.

The extrapolation procedure was verified using simulated positrons. Reconstructed tracks were extrapolated into the calorimeter and compared to the *true* position of impact of the positron on the calorimeter. Figure 44 shows the results of this study and confirms that the Runge-Kutta extrapolation is working well.

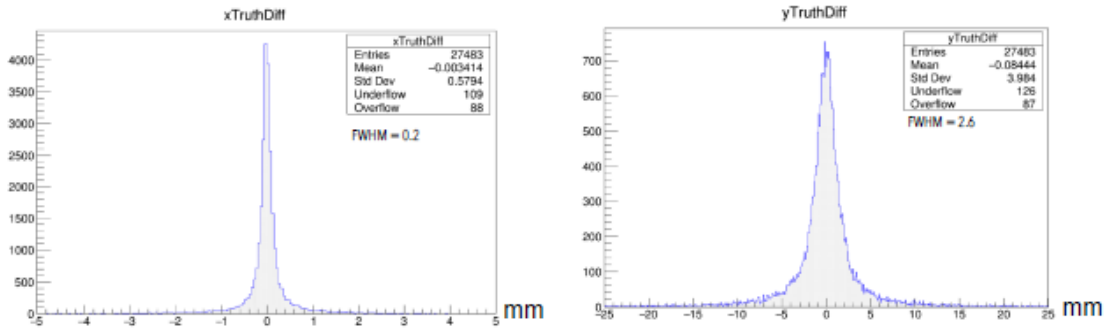

Figure 44: Comparison of extrapolated and true track impact positions on calorimeter.

In the simulation the tracker and calorimeter are in their nominal positions and no offsets between extrapolation and truth can be seen. The extrapolation algorithm is seen to be performing well. For completeness the impact position of the extrapolated track on the calorimeter is shown in Figure 45.

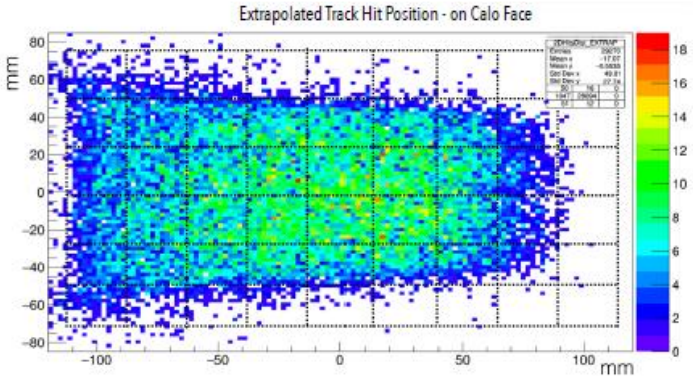

Figure 45: Impact position of extrapolated tracks on the calorimeter face in the simulation.

Comparison of extrapolated tracks with reconstructed calorimeter clusters is complicated by the dependence of cluster position on the number of crystals used in reconstructing the cluster. For example Figure 46 shows that for single crystal clusters the positions are simply put at the crystal centre.

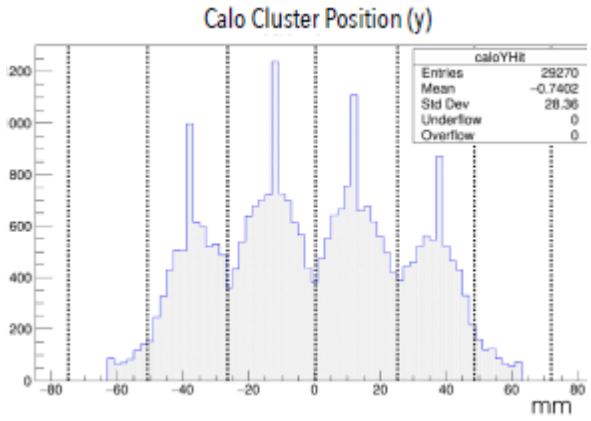

Figure 46: Reconstructed calorimeter cluster positions for single crystal clusters.

On the other hand, if several crystals have contributed to a cluster, the cluster position tends to be at the crystal edges (Figure 47).

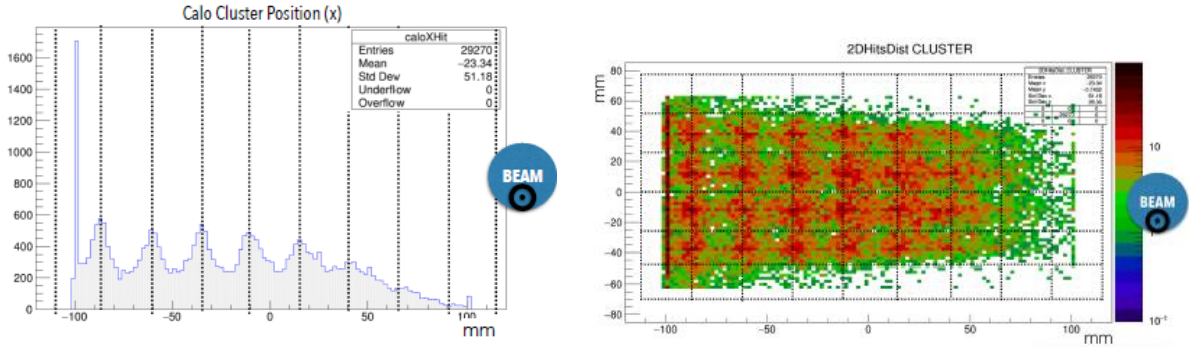

Figure 47: Reconstructed calorimeter positions for multi-crystal clusters.

The result of these effects is that even in simulation with perfectly aligned detectors the horizontal difference between extrapolation and reconstructed cluster is offset from zero (Figure 48).

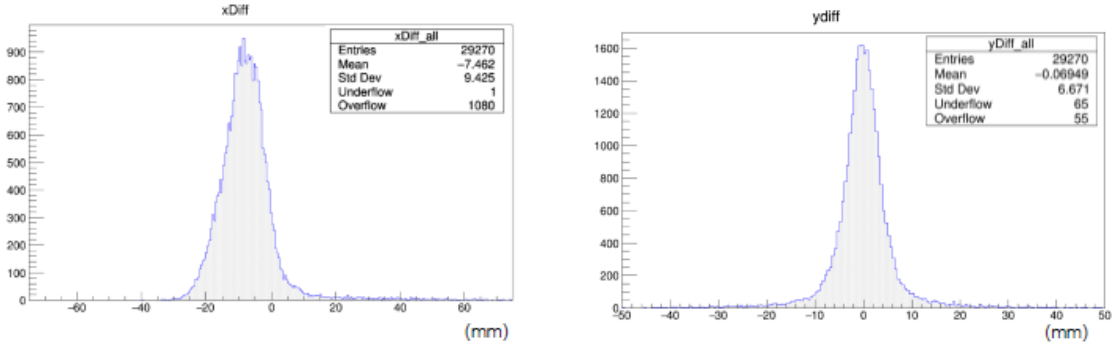

Figure 48: Horizontal and vertical offset between reconstructed calorimeter clusters and extrapolated tracks.

The extrapolation algorithm has also been run on real data, yielding the plots shown in Figure 49. Firstly, a comparison between track momentum and cluster energy (Figure 49) shows a clear difference between genuine positrons and “lost muons”.

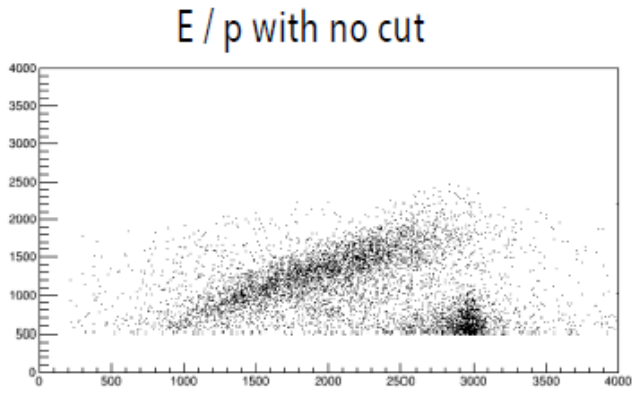

Figure 49: Real data comparison of calorimeter energy and track momentum.

For the real data reconstructed calorimeter cluster positions are shown in Figure 50, showing clear peaks at the crystal centres. The bottom right plot shows the impact positions of track extrapolations on the calorimeter front face.

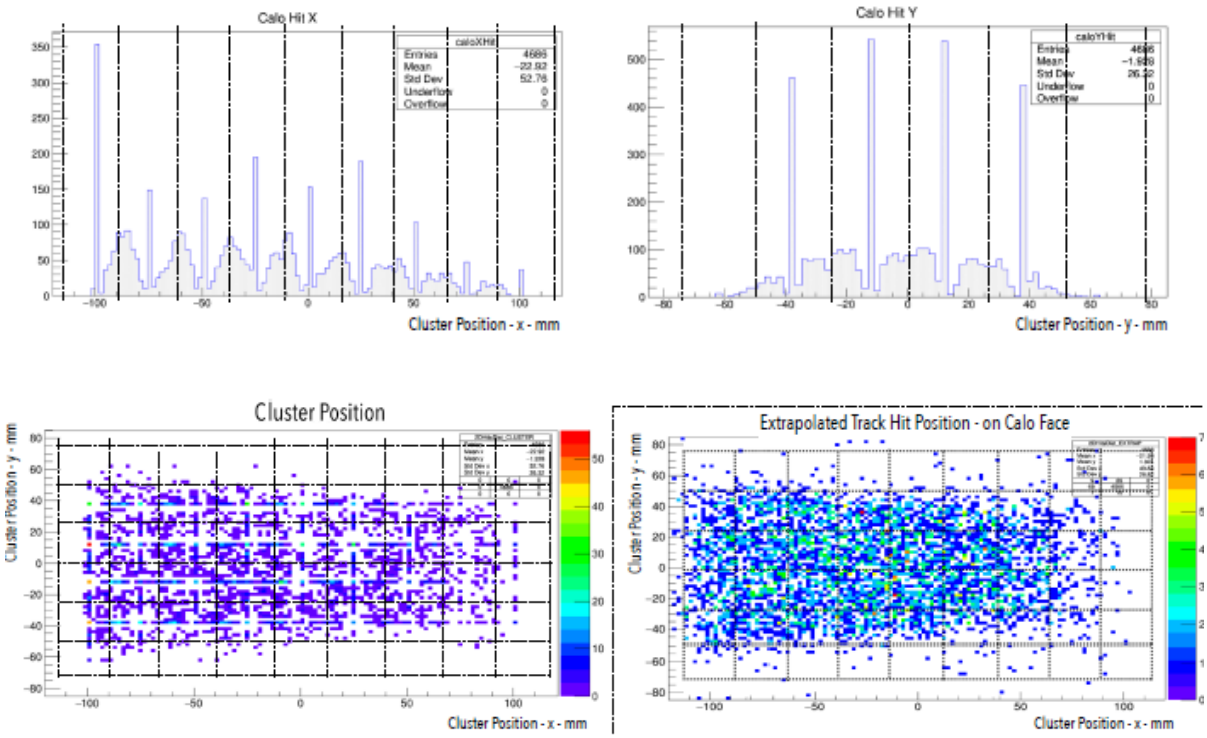

Figure 50: Reconstructed cluster positions in real data. The bottom right plot shows extrapolated track impact positions on the calorimeter front face.

Comparison of data with simulation is starting to yield information about the relative tracker and calorimeter alignment. Figure 51 shows the horizontal and vertical offsets in simulation and in real data. It is clear that the real data has a vertical offset of ~2.7 mm not seen in the simulation. This is a real misalignment that will be corrected for in future analyses.

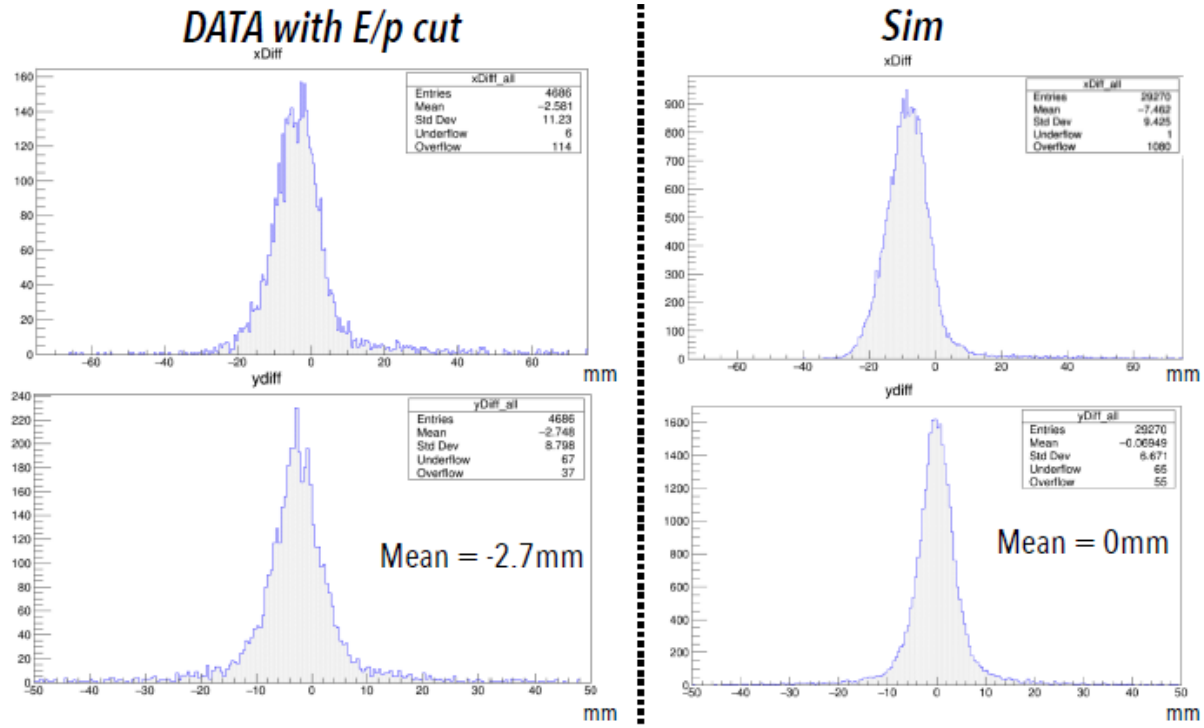

Figure 51: Horizontal and vertical offsets between extrapolated tracks and calorimeter clusters in real data and in the simulation.

Further work is currently ongoing to understand the source of all discrepancies, particularly in terms of the incident angle of the track on the calorimeter. For example, Figure 52 shows the dependence of the horizontal offset between cluster and extrapolation as a function of incoming track angle.

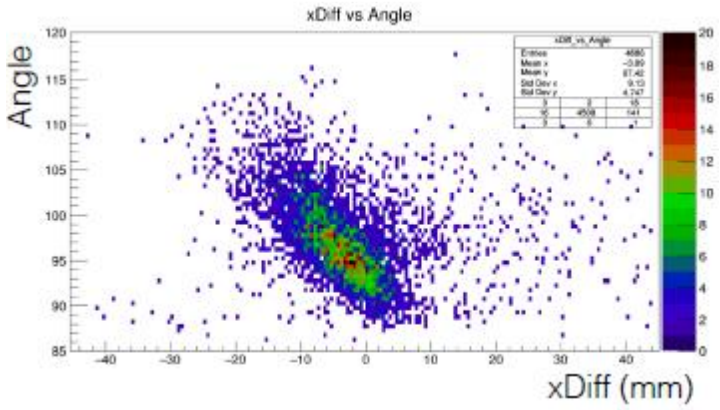

Figure 52: Dependence of horizontal extrapolation/cluster offset on the incident track angle.

7. Conclusions.

The g-2 experiment is now entering a truly exciting phase, during which physics data is being taken and will definitively answer the question whether the muon anomalous magnetic moment is described by our current understanding of physics at the small scale: The Standard Model.

The tracking detectors for the g-2 experiment have been built on time and have been installed into the g-2 experiment. They have been fully tested both in Liverpool and upon arrival at Fermilab. Their performance has been characterised in many tests prior to insertion in the experiment.

The trackers are fully functional and will fulfill their designated roles in the physics programme of E989. The systems needed to operate the detectors (gas, water cooling) are in place and operating as required. The readout for the trackers is fully functioning, as is the tracker DAQ system. Work is ongoing to further improve the diagnostic histograms available to shift personel. The tools needed for beam diagnostic physics studies are in place, as are those necessary for calorimeter pileup and gain studies.

We are now entering the exciting phase of the experiment where all the hard work devoted to producing the detectors and their associated software packages will pay dividends in the forthcoming physics results.

Finally, it should be mentioned that much of the work described here would not have been possible without funding from the MUSE project. Most of the people pictured in the various figures have benefitted in one way or another from the MUSE funding of this project.